

Slow dynamics in a turbulent von Kármán swirling flow

A. de la Torre^{1,*} and J. Burguete^{1,†}

¹Departamento de Física y Matemática Aplicada
Universidad de Navarra, P.O.Box 177, E-31080 Pamplona, Spain

We present an experimental study of a turbulent von Kármán flow produced in a cylindrical container using two propellers. The mean flow can be considered stationary up to $Re = 10^4$, where a bifurcation takes place. The new regime breaks some symmetries of the problem, and is time-dependent. The axisymmetry is broken by the presence of equatorial vortices with a precession movement, being the velocity of the vortices proportional to the Reynolds number. The reflection symmetry through the equatorial plane is broken, and the shear layer of the mean flow appears displaced from the equator. These two facts appear simultaneously. In the exact counterrotating case, a bistable regime appears between both mirrored solutions and spontaneous reversals of the azimuthal velocity are registered. This evolution can be explained using a simple two-well potential model with additive noise. A regime of pseudo-stochastic resonance is observed when a very small input signal is applied.

PACS numbers: 05.45.-a, 47.27.-i, 47.32.-y, 47.65.-d

Introduction - Turbulent flows are ubiquitous in nature: ranging from small scales (heart valves, turbulent mixing) to very large scales (clouds, tornadoes, oceans, earth mantle, the sun and other astrophysical problems), turbulence is present in many applied and fundamental physical problems[1]. But, in spite of the attention it has received, there are still many open questions: the emergence of coherent structures, as vortices, in fully developed turbulence or the rise of different bifurcations on the mean flow[2].

Here we will focus in a particular configuration, the von Kármán swirling flow, where two different propellers are rotating inside a cylindrical cavity. These flows has been studied analytically[3, 4], numerically [5, 6, 7] and experimentally [8, 9, 10]. Recently it has been shown that they can present multistability and memory effects[11]. These von Kármán flows have been used in magnetohydrodynamics (MHD) experiments looking for the dynamo action, with recent successful results [12] and with a very rich dynamics of the magnetic field [13]. Because of turbulence, the whole MHD problem can not be studied numerically: a usual approach is to deal with stationary mean flows in the so called kinematic dynamo scheme. Although these numerical studies have been used to predict thresholds of the dynamo action[17, 18, 19], real flows can present slow dynamics that can not be neglected and should be taken into account in the numerical codes. On the experimental side, these slow varying flows could produce similar dynamics in the magnetic field.

In this paper we will focus on the slow dynamics that appear for very large Re numbers. The flow presents a non-trivial alternation between two states that break symmetries of the problem. This dynamics, which can be assimilated to a Langevin system, present intermittency, with a classical exponential escape time, and stochastic resonance.

Experimental setup - The experimental volume (Fig.1) is a closed, horizontal cylinder whose diameter $D = 2R =$

20cm is fixed and the height H can be modified continuously. Two propellers are placed at both ends, with radius $R_{prop} = 9\text{cm}$ and 10 curved blades, each blade with a height of 2 cm and a curvature radius of 4.5 cm. Using the standard cylindrical coordinate system, the north N (resp. south S) propeller placed at $z = H/2$ (resp. $z = -H/2$) has negative (resp. positive) azimuthal velocity. The propellers are impelled by two independent

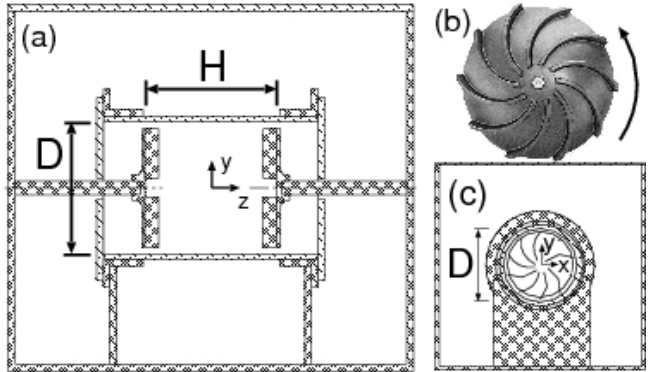


FIG. 1: Experimental setup. (a) Horizontal cylinder with the propellers, inside the tank. The north propeller is at $z = H/2$ and the south is at $z = -H/2$. (b) Photograph of the propeller. (c) Scheme of the south propeller viewed from the equatorial plane. The rotation sense with the convex side sets the azimuthal velocity as positive.

motors of 3 kW total power, allowing a rotation frequency in the range $f = 0 - 20$ Hz. The frequency of the motors is controlled with a waveform function generator and a PID servo loop control. The cylinder is placed inside a tank of 150 l of volume in order to avoid optical problems and to assure the temperature stability. The fluid used is water at 21°C.

The measurement of the velocity field is performed using a LDV system (with a chosen spatial resolution of 1cm and temporal resolution up to 100 kHz) and a PIV

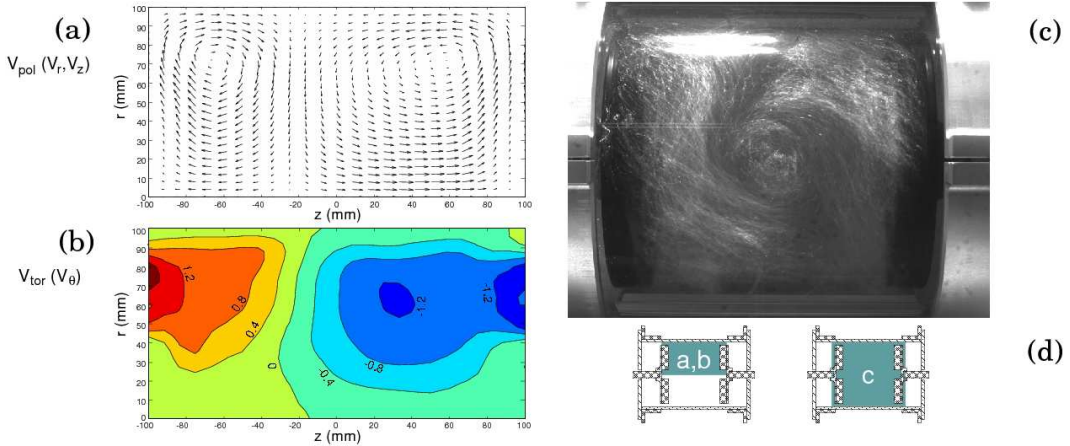


FIG. 2: (Color online) (a) Stream-vectors V_r, V_z in the plane $\theta = 0$. (b) Contourplot of V_θ . The north propeller is on the right, the south propeller on the left. (c) Vortex visualized with air bubbles. (d) Gray zones indicating the regions where the figures (a,b,c) were obtained in the cell.

system (spatial resolution of 1 mm and temporal resolution of 15 Hz). The LDV system allows the measurement of two components of the velocity field (axial v_z and azimuthal v_θ), while the radial component (v_r) is obtained by mass conservation. The velocity field obtained in this way is consistent with the PIV measurements in an axial, horizontal plane ($\theta = 0$). Both techniques are based on the displacement of small particles ($14\mu\text{m}$, $\rho = 1.65\text{g}/\text{cm}^3$) inside the bulk of the fluid.

In our experimental setup three parameters can be modified. The first one is the Reynolds number $Re = RV_{prop}/\nu$, defined using the propeller's rim velocity $V_{prop} = 2\pi R_{prop}f$. This number can be varied continuously in the range $Re \sim 10^3 - 10^6$. The second one is the aspect ratio of the experimental volume, $\Gamma = H/D$, set to 1 in this experiment. The last one is the frequency disymmetry, defined as $\Delta = (f_N - f_S)/(f_N + f_S)$, where f_N and f_S are the frequencies of each propeller, north and south. This parameter is varied in the range $|\Delta| < 0.1$.

Results - For the Re range explored, the flow is in fully-developed turbulence regime. The mean flow $V = \langle v \rangle = (V_r, V_\theta, V_z)$ represented in Fig.2(a,b) is obtained with the LDV system, averaging velocity series longer than 300 times the period of the propeller. The measurement is done in the plane $\theta = 0$ with $Re = 3 \cdot 10^5$ and $\Delta = 0$. The flow is divided into two toroidal cells, each of them following its propeller (positive azimuthal velocity in the south, negative in the north). In each cell, the flow is aspirated through the axis towards the propellers, where it is ejected to the walls. The flow then returns along the cylinder's wall, approaching the axis near the equatorial plane. Using PIV measurements, the instantaneous field can be obtained, and no traces of the mean flow are observed. This is due to the high turbulence rate (rms value over the mean value) which vary between 60 – 150%, depending on the spatial position and the velocity component measured.

This mean flow does not preserve the symmetry around the equator (a π rotation around any axis in the $z = 0$ plane, i.e. R_π symmetry). In the case presented in figure 2(a,b) the cell near the north propeller is bigger than the south one. The broken symmetry is recovered when the mirror state (south cell bigger than the north cell) is considered. Each state (labeled as 'north' N or 'south' S depending on which cell is the *dominant* one, i.e. bigger) are equally accessible when the system starts from rest. This disymmetry is in contradiction with other works[8] in which the R_π symmetry is observed (i.e., the frontier between the two rolls is always in the plane $z = 0$), probably due to the presence of baffles or inner rings, which would enforce this condition. Other experiments at much slower Reynolds numbers[10] ($Re \leq 600$) have shown that the axisymmetry can be broken producing near heteroclinic orbits, but always preserving the R_π symmetry.

When larger tracers (air bubbles) are used, coherent structures as vortices (Fig.2c) are visualized. These structures mostly relay in the dominant cell, so the azimuthal velocity of the vortices are directly related with the azimuthal velocity of the dominant cell. These vortices have a characteristic size $D_{vortex} = 5\text{cm}$ and they appear simultaneously to the disymmetry of the mean flow. Previous works in similar configurations [7] showed the formation of a static vortex in the equatorial plane ($z = 0$) for much lower Re , inaccessible with the present configuration.

The state N or S of the system can be characterized using different variables. One is the position of the frontier z_0 , defined as the z position in where $V_\theta = 0$ (in Fig.2b, $z_0 \sim -20 \text{ mm}$). Another possibility is measuring V_θ^{eq} , the mean azimuthal velocity at an equatorial point near the wall ($r = 0.9R, z = 0$) with the LDV system (in Fig.2b, $V_\theta^{eq} \sim -0.4 \text{ m/s}$). This mean velocity is stable in time and proportional to the propeller's rim velocity. For

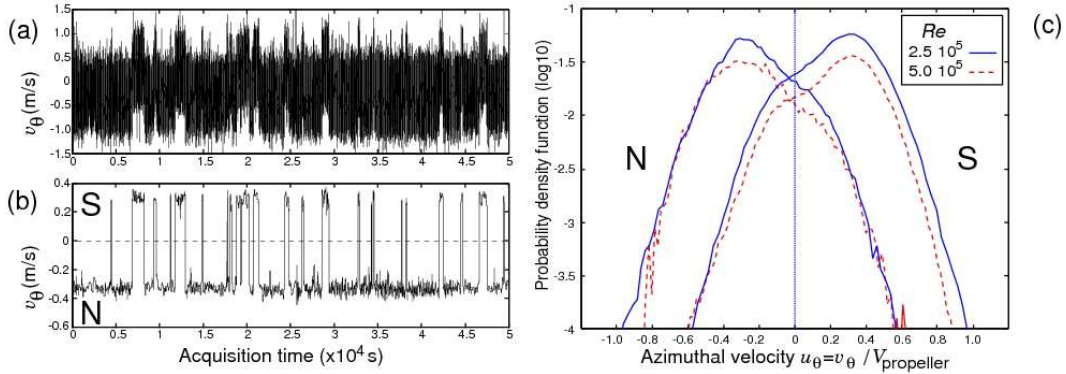


FIG. 3: (Color online) Inversions of the azimuthal velocity at a point near the wall in $z = 0$ for $\Delta = 0$, $Re = 3 \cdot 10^5$ (a) without filter, (b) with a low band-pass filter. (c) PDF of u_θ for each state (north or south) obtained for various Re .

$Re < 10^4$ we find that the normalized azimuthal velocity ($U_\theta = V_\theta^{eq}/V_{prop}$) is nearly null so the mean flow is almost symmetric. As the Re is increased the disymmetry becomes more notorious, until a plateau ($U_\theta = const$) is reached for $Re > 10^5$.

For this range of Re the system can spontaneously jump from one state to the other (*inversions*). In Fig.3(a) the instantaneous azimuthal velocity of the equator is plotted versus time ($t_{acq} = 2.4 \cdot 10^5$ $T_{prop} = 5 \cdot 10^4$ s ~ 14 h) for $Re = 2.7 \cdot 10^5$, $\Delta = 0$. The typical transition time is about 10 s, while the time between inversions can vary from minutes to hours. This time scales are much slower than the period of the propeller ($T_{prop} = 0.2$ s). Fig.3(c) shows the probability density function (PDF) of the normalized instantaneous azimuthal velocity ($u_\theta = v_\theta/V_{prop}$) for the two states: north (with negative most probable u_θ) and south (with positive most probable velocity). Each distribution (p_N or p_S) can be described as the superposition of two gaussians:

$$p_{N,S}(u_\theta) = G_0 + G_{N,S} = \frac{A_0}{\sqrt{2\pi}\sigma_0} \exp\left(-\frac{u_\theta^2}{2\sigma_0^2}\right) + \frac{A_{N,S}}{\sqrt{2\pi}\sigma_{N,S}} \exp\left(-\frac{(u_\theta - u_{N,S})^2}{2\sigma_{N,S}^2}\right) \quad (1)$$

with $A_0 + A_{N,S} = 1$. Both distributions p_N and p_S share the same properties: one of the gaussians G_0 has zero mean, while the other $G_{N,S}$ is centered around a finite value ($|u_N| = |u_S| \neq 0$) that increases slightly with the Re number. The amplitudes A_0 and $A_{N,S}$ have a stronger dependency on the Re (Fig.4). For low Re the PDF are nearly gaussians ($A_0 \simeq 1$) while for large Re (plateau) the non-symmetric gaussian becomes dominant $A_{N,S} \gg A_0 \neq 0$. The zero mean gaussian G_0 is due to residues of the symmetric flow and the other gaussian $G_{N,S}$ is related to the displacement of the vortices around the equator.

Some of the characteristics of the slow dynamics presented can be recovered using a third-order Langevin

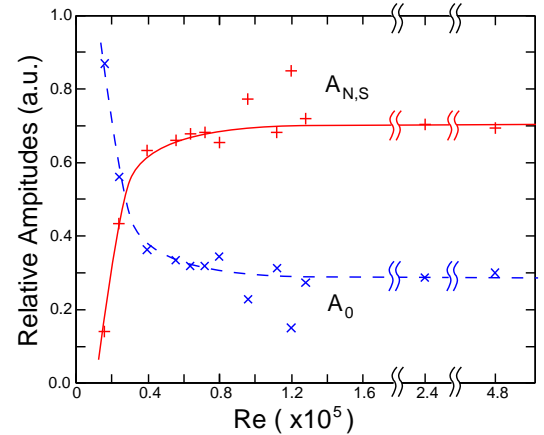


FIG. 4: (Color online) Amplitude of the gaussians in Eq.1 vs Re . The lines are only plotted to indicate the trend and are not obtained from any fitting.

equation (a two-well potential):

$$\dot{u}_\theta = \epsilon u_\theta - u_\theta^3 + \sqrt{2B} \xi(t) \quad (2)$$

where $\xi(t)$ is a noise distribution (in our case will be the turbulence) and B the noise level. The fluctuations allow the system to jump from one well to the other with a characteristic escape time that can be computed. The distribution of these *residence time* follows an exponential decay law (Kramer's scape rate [14, 15]) for different noise distributions (Gaussian or Levy noise[16]):

$$\rho(t) \sim e^{-t/T_0} \quad (3)$$

where T_0 is related to the intensity of the noise distribution. The scape rate distribution in our problem agrees with this description, with a typical value of $T_0 = 10^3$ s.

It is well known that a Langevin system can present stochastic resonance[20]. In order to test this possibility in our experiment, we applied two different forcings (static and harmonic) on the Δ parameter ($\Delta =$

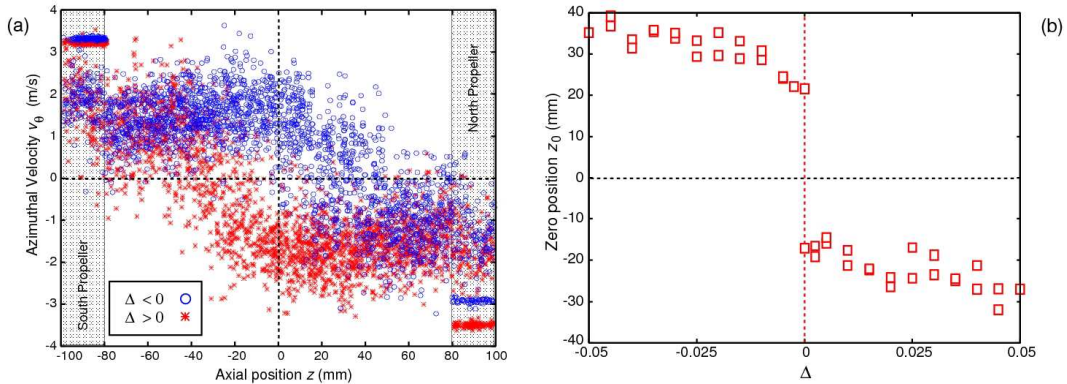


FIG. 5: (Color online) (a) v_θ of coaxial points near the wall for $\Delta \neq 0$. The position where the mean velocity is zero is labeled as the frontier position (z_0). (b) Position of the frontier (z_0) varying the difference between the propellers' frequency (Δ). The system presents a bistability at $\Delta = 0$.

$$\Delta_0 \cos(\omega t):$$

$$\dot{u}_\theta = \epsilon u_\theta - u_\theta^3 + \sqrt{2B} \xi(t) + \kappa \Delta_0 \cos(\omega t) \quad (4)$$

The static forcing ($\omega = 0$, $\Delta_0 \neq 0$) was applied in order to obtain the minimum amplitude that can induce an inversion in the experiment. Fig.5a represents $v_\theta|_{r=0.9R}$ versus z for $\Delta \simeq \pm 0.05$, $Re \sim 4 \cdot 10^5$. As it was expected, when a disymmetry is forced into the system a spatial disymmetry is observed ($\Delta_0 \simeq \pm 0.05 \Rightarrow z_0 \simeq \mp 30\text{mm}$). In Fig.5b z_0 is represented vs Δ . No hysteresis is found up to our precision as even a change of $\Delta \sim 0.0025$ makes the system jump between both states.

When the harmonic forcing is induced, preliminary results show how for low ω only a small amplitude in the input signal is needed to obtain the resonance of the system: Periodic inversions are observed with the same frequency of the forcing. In the range $10^{-2} > \omega/\omega_{prop} > 10^{-3}$ it is necessary to increase Δ to observe the synchronicity. For higher ω , the system can not follow the forcing: the inertia of the flow limits the response time of the inversion $T_{res} \sim 20\text{s} = 10^2 T_{prop}$.

Conclusions - We have presented experimental evidence of a bifurcation in a turbulent system that breaks symmetries and produces slow dynamics. Two possible mirror states are equally accessible, with random (natural) or periodic (induced) inversions. The slow dynamics can be characterized using a very simple Langevin model, even if the base flow is in a fully developed turbulence regime. Finally, when a very weak amplitude (0.25%) input modulation is applied to the system, a pseudo-stochastic resonance appear in the turbulent flow. One open question is either these natural inversions could be present in dynamo experiments for very long temporal series ($T_0 \simeq 1000\text{s}$) when $\Delta = 0$.

Acknowledgements - We are grateful to Jean Bragard and Diego Maza for fruitful discussions. This work has been supported by the Spanish government (research projects FIS2004-06596-C02-01 and UNAV05-33-

001) and by the University of Navarra (PIUNA program). One of us, AdlT, thanks the “Asociación de Amigos” for a post-graduate grant.

* Electronic address: admonguio@alumni.unav.es

† Electronic address: javier@fisica.unav.es

- [1] U. Frisch, *Turbulence* (Cambridge University Press, 1995).
- [2] P. Holmes, J.L. Lumley, G. Berkooz, *Turbulence, Coherent Structures, Dynamical Systems and Symmetry* (Cambridge University Press, 1996).
- [3] T. von Kármán, Z. Angew Math. Mech **1**, 233 (1921).
- [4] P. Zandbergen, D. Dijkstra, Ann. Rev. Fluid Mech. **19**, 465 (1987).
- [5] W. Z. Shen, J. Norensen, J. Michelsen, Phys. Fluids **18**, 064102 (2006).
- [6] C. Nore, L. M. Witkowski, E. Foucault, J. Pecheux, O. Daube, P. Le Quere, Phys. Fluids **18**, 054102 (2006).
- [7] C. Nore, L. S. Tuckerman, O. Daube, S. Xin, J. Fluid Mech. **477**, 51 (2003).
- [8] F. Ravelet, A. Chiffaudel, F. Daviaud, J. Leorat, Phys. Fluids **17**, 117104 (2005).
- [9] L. Marie, J. Burguete, F. Daviaud, J. Leorat, Eur. Phys. J B **33**, 469 (2003).
- [10] C. Nore, F. Moisy, L. Quartier, Phys. Fluids **17**, 064103 (2005).
- [11] F. Ravelet, L. Marie, A. Chiffaudel, F. Daviaud, Phys. Rev. Lett. **93**, 164501 (2004).
- [12] R. Monchaux *et al.*, Phys. Rev. Lett. **98**, 044502 (2007).
- [13] M. Berhanu *et al.*, submitted to Europhys Lett (2007).
- [14] H. Kramers, Physica A **7**, 284 (1940).
- [15] P. Hänggi, P. Talkner, Rev. Mod. Phys. **62**, 251 (1990).
- [16] A. Chechkin, V. Gonchar, J. Klafter, R. Metzler, Europhys. Lett. **72**, 348 (2005).
- [17] A. Gailitis *et al.*, Phys. Rev. Lett. **84**, 4365 (2000).
- [18] R. Stieglitz and U. Müller, Phys. Fluids **13** 561 (2001)
- [19] F. Petrelis *et al.* Phys. Rev. Lett. **90** 174501 (2003)
- [20] L. Gammaitoni, P. Hänggi, P. Lung, F. Marchesoni, Rev. Mod. Phys. **70** 223 (1998)